

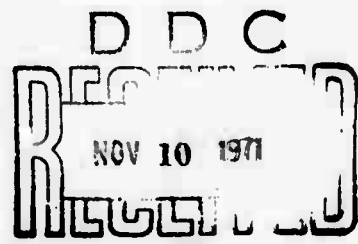
R71-42
30 OCTOBER 1971

AD732454

**THIRD QUARTERLY TECHNICAL REPORT
(1 JULY-30 SEPTEMBER 1971)**
**USE OF ELECTRON BEAM GUN
FOR HARD ROCK EXCAVATION**

Submitted to

**U.S. Department of Interior
Bureau of Mines
Twin Cities Mining Research Center
Twin Cities, Minnesota
Contract No. H0110377**



Sponsored by

**Advanced Research Projects Agency
ARPA Order No. 1578
Program Code OF010**

DISTRIBUTION STATEMENT A
Approved for public release;
Distribution Unlimited

Westinghouse

**Missile Launching & Handling Department
Sunnyvale, California**

Reproduced by
**NATIONAL TECHNICAL
INFORMATION SERVICE**
Springfield, Va. 22151

The views and conclusions contained in this document are those of the authors and should not be interpreted as necessarily representing the official policies, either expressed or implied, of the Advanced Research Projects Agency or the U. S. Government.

Distribution of this document is unlimited.

44

UNCLASSIFIED

Security Classification

DOCUMENT CONTROL DATA - R & D

(Security classification of title, body of abstract and indexing annotation must be entered when the overall report is classified)

1. ORIGINATING ACTIVITY (Corporate author) WESTINGHOUSE ELECTRIC CORPORATION Missile Launching & Handling Department Hendy Avenue, Sunnyvale, California		2a. REPORT SECURITY CLASSIFICATION Unclassified
		2b. GROUP ---
3. REPORT TITLE USE OF ELECTRON BEAM GUN FOR HARD ROCK EXCAVATION —Third Quarterly Technical Report		
4. DESCRIPTIVE NOTES (Type of report and inclusive dates) Quarterly Technical Report (1 July - 30 September 1971)		
5. AUTHOR(S) (First name, middle initial, last name) David R. Nixon; Dr. Berthold W. Schumacher		
6. REPORT DATE 30 October 1971	7a. TOTAL NO. OF PAGES 36	7b. NO. OF REFS 7
8. CONTRACT OR GRANT NO H0110377	9a. ORIGINATOR'S REPORT NUMBER(S) WEC R 71-42	
9. PROJECT NO ARPA Order No. 1578	9b. OTHER REPORT NO(S) (Any other numbers that may be assigned this report)	
10. DISTRIBUTION STATEMENT Distribution of this document is unlimited.		
11. SUPPLEMENTARY NOTES	12. SPONSORING MILITARY ACTIVITY Advanced Research Projects Agency Washington, D.C. 20401	

13. ABSTRACT

Because of alignment problems, output power of the electron beam gun (EBG), not funded by the contract, has been restricted to about 12 kW. Installation of beam position sensors and a closed-loop beam positioning system should permit continuous operation at the desired 36-kW level. But these installations will require two months, and this will mean a delay in the start of the field tests. In-plant tests of the EBG carriage show compliance with the specification, except for velocity irregularities and hydraulic system overheating. The addition of a heat exchanger should solve the overheating problem. Thermal stress calculations of the Second Quarterly Report have been repeated for a reduced thermal diffusivity. The results are similar except that the width of the stressed region is reduced by 15 to 20 percent. Computer plots of the probability density show the points at which cracks are most likely to start.

UNCLASSIFIED
Security Classification

14 KEY WORDS	LINK A		LINK B		LINK C	
	ROLE	WT	ROLE	WT	ROLE	WT
Electron Beam Tunneling Mining Rocks Minerals Excavation Fracture Mechanics Evaporation Melting Thermal Stress						

Distribution of this document is unlimited.

R 71-42
30 October 1971

THIRD QUARTERLY TECHNICAL REPORT
(1 July - 30 September 1971)

USE OF ELECTRON BEAM GUN
FOR HARD ROCK EXCAVATION

Contract No. H0110377

ARPA Order No. 1578
Program Code OF010

Effective Date of Contract: 11 December 1970

Contract Expiration Date: 10 December 1971

Amount of Contract: \$240,000 (CPFF)

Principal Investigator: D. R. Nixon
(408) 735-2271

Project Scientist: Dr. B. W. Schumacher
(412) 256-3522

WESTINGHOUSE ELECTRIC CORPORATION
Missile Launching & Handling Department
Sunnyvale, California

The views and conclusions contained in this document are those of the authors and should not be interpreted as necessarily representing the official policies, either expressed or implied, of the Advanced Research Projects Agency or the U. S. Government.

Details of illustrations in
this document may be better
studied on microfiche

Distribution of this document is unlimited.

FOREWORD

This quarterly technical report, covering the period 1 July - 30 September 1971, was prepared by the Westinghouse Electric Corporation.

The research reported in this document is supported by the Advanced Research Projects Agency of the Department of Defense and is monitored by the Bureau of Mines under Contract H0110377.

CONTENTS

<u>Section</u>		<u>Page</u>
	ILLUSTRATIONS	iv
	TABLE	iv
	SUMMARY	v
1	INTRODUCTION	1-1
2	ELECTRON BEAM GUN AND SUPPORT EQUIPMENT	2-1
	2.1 Electron Beam Gun and Controls	2-1
	2.2 Support Equipment	2-6
	2.2.1 Carriage Test Procedure	2-6
	2.2.2 Carriage Test Results	2-7
	2.2.3 Conclusions and Recommendations	2-9
3	FIELD TESTS	3-1
4	THEORETICAL STUDIES	4-1
	4.1 Piercing Rock with the Electron Beam	4-1
	4.2 Temperature Distribution	4-5
	4.3 Rock Failure	4-8
5	LABORATORY TESTS	5-1
6	REFERENCES	6-1
	Document Control Data - R&D	

ILLUSTRATIONS

<u>Figure</u>		<u>Page</u>
2-1	Cross-Section Sketch of Electron Beam Gun	2-2
2-2	Front End of Electron Beam Gun Facing Water-Cooled Beam Catcher Used for Initial Alignment	2-4
2-3	Electron Beam Gun in Front of Siltstone (Copper Ore) Before and After Piercing	2-5
2-4	Axis Orientation and Rotational Modes for Electron Beam Gun	2-8
2-5	EBG Carriage — X-Axis Actuation Velocities	2-10
2-6	EBG Carriage — Y-Axis Actuation Velocities	2-11
2-7	EBG Carriage — Pitch Actuation Velocities	2-12
2-8	EBG Carriage — Yaw Actuation Velocities	2-13
4-1	Failure Probability per Unit Area Caused by Tensile Stress	4-10

TABLE

<u>Table</u>		<u>Page</u>
2-1	Comparison of 36-kW EBG and Mock-Up EBG	2-7

SUMMARY

PURPOSE

Westinghouse is seeking field operating data with which to verify and extend theoretical and laboratory data on the feasibility of employing the electron beam gun (EBG) to satisfy the needs for removal of hard rock. These practical data will provide initial definition of equipment configuration and applicable modes of operation.

TECHNICAL PROBLEMS

Support Equipment. Westinghouse is modifying its existing 36-kW EBG and will provide support equipment necessary for field operation.

Field Tests. This program involves the use of the 36-kW EBG to determine whether laboratory test data on melting rates, breakage mechanisms, etc., can be extrapolated to predict field performance. The field site being selected will provide working faces representative of a large, relatively unfractured rock mass. During field tests, Westinghouse will determine the techniques and procedures, such as cutting pattern, gun tracing speed, and method of cut, required to produce the optimum excavation rate.

Theoretical Studies. Westinghouse is studying the effects of different heating geometries and heating rates on stress distribution patterns and associated breakage phenomena. Westinghouse will also attempt to develop theoretical models for an optimum mode of operation.

Laboratory Tests. Westinghouse is conducting laboratory tests to support theoretical work and field experiments and to extend the use of the EBG to different rock types.

Systems Analysis Study. Westinghouse will evaluate the feasibility of developing a hard rock excavation system using the EBG as the prime source of power for rock fragmentation.

TECHNICAL RESULTS

This report covers effort performed during the third quarter of the contract. This work is a continuation of that reported in the second quarterly report (Ref. 3)*. Work was performed in two of the five areas summarized above; the systems analysis study will not become active until the field test effort has been completed and evaluated. A sixth area (not included in the contract) is the completion of the 36-kW EBG and its conversion from a laboratory model to a field test version.

Support Equipment. The gun carriage with an EBG mockup was tested in-plant for compliance with Westinghouse Specification S71-1 and to calibrate the carriage hydraulic system flow controls. The carriage performs as required by the specification except for irregularities in velocity control and the problem of hydraulic system overheating. The addition of a heat exchanger should solve the overheating problem.

Field Tests. Field test planning effort was essentially completed during the second quarter, and there was no activity this quarter, pending arrival of the EBG modified for rock cutting in the field.

Because of beam alignment problems, the output power of the EBG has been restricted to about 12 kW. Installation of beam position sensors and a closed-loop beam positioning system should permit continuous operation at the desired 36-kW level. But these installations will require two months, and this will mean a delay in the start of the field tests.

Theoretical Studies. The effects of several beam-degrading processes, neglected in the First Quarterly Report, were estimated and found to be quite small for the power levels and distances involved. Thermal stress calculations, using the mathematical model in the Second Quarterly Report, were repeated for an assumed thermal diffusivity of half the original value. The isostress plots have nearly the same shape, but the width of the stressed region is reduced by 15 to 20 percent. There is no significant decrease in the maximum tensile stress.

*See list of references in Section 6.

Computer plots of the failure probability density were obtained for piercing times of 4 to 300 seconds with a 9-kW beam at a 1/2-inch standoff distance. The probability that the rock will crack somewhere is essentially unity for each of the piercing times considered. The plot contours show the points at which the cracks are most likely to start.

Laboratory Tests. No laboratory tests were performed during the third quarter.

DoD IMPLICATIONS

The primary DoD implication of a successful field test program is the potential to fragment and remove hard rock from any location without degrading the structural integrity of the parent rock from which it was removed.

Upon completion of the appropriate development program, the EBG system could be applied to rock-removal systems for programs such as

- Sanguine
- Cheyenne Mountain
- Minuteman
- Safeguard
- AEC testing

and probably a number of other applications. In addition, an operational EBG system would have applications to the programs of the Department of Transportation and other agencies.

It should be stressed, however, that a considerable development program will be required after the assumed successful field tests before an operational system can be delivered.

IMPLICATIONS FOR FURTHER RESEARCH AND DEVELOPMENT

Westinghouse believes that the current field test program will demonstrate the potential of the EBG for hard-rock fragmentation. Based on the successful completion of these tests, additional research and development effort can be envisioned in the following areas:

1. Additional tests in various types of open quarries and in underground mines.
2. Evaluation of EBG in conjunction with existing mining and tunneling equipment and as part of a total system design.
3. Improved knowledge of rock failure mechanisms.
4. Investigation of the use of ion beams with their reduced shielding requirements.
5. Increase in power and/or increase in electron acceleration voltage.
6. Real-time predictions of geologic conditions using existing optical and acoustic sensing technologies.

These areas of continuing investigation will augment a product development program that is aimed at the achievement of a system to satisfy government and industrial needs for hard-rock removal.

1. INTRODUCTION

Laboratory tests conducted by Westinghouse have shown that the electron beam gun (EBG) may be a promising tool for use in hard-rock excavation (Ref. 1)*. These tests have been conducted on small, unconstrained, laboratory test specimens weighing a few hundred pounds. Under the present contract, field tests are to be conducted to study the electron beam process on a semi-infinite, constrained rock mass, such as might be encountered in mining or tunneling operations.

The objectives of the electron beam gun evaluation program are:

1. To obtain field operating data.
2. To determine the effectiveness and economic feasibility of the electron beam gun compared with conventional methods of hardrock excavation.
3. To determine practical optimums for equipment configuration and modes of operation.

In support of the foregoing effort, laboratory experiments and theoretical studies are being conducted to compute and, if possible, to predict the thermal stresses and the resultant rock fragmentation for various cutting strategies and electron beam parameters in different types of rock.

*See list of references in Section 6.

2. ELECTRON BEAM AND SUPPORT EQUIPMENT

2.1 ELECTRON BEAM GUN AND CONTROLS

The electron gun is described in some detail in the First Quarterly Report (Ref. 2). Figure 2-1 is included here for reference purposes. It shows the long beam transfer column, which is unique to this rock cutting machine.

Several problems were encountered in starting up this system, and they had to be solved. Because of scattered electrons, overheating occurred, particularly in a ball valve that closes off the gun proper from the atmosphere when the vacuum pumps for the transfer column are not in operation. It is located to the right of Lens 1 in Figure 2-1, but not shown in the figure. Replacing the original 1-inch-diameter valve by a 2-inch-diameter valve solved this problem.

In several laboratory tests, the machine has pierced and cut into stationary blocks of rock. With the beam in a horizontal position, the machine was traversed vertically up and down the rock face. The output power had to be restricted to about 12 kW because of a slow drift encountered in the beam alignment system. No burn-out of the exit nozzle occurred as long as the beam remained aligned. But since the beam-position sensors near the front end of the gun (see Figure 2-1) have not yet been installed, there is presently no control over the beam position during cutting. After approximately an hour of cutting time, the nozzles have burned out to a degree that replacement became necessary. Usually the burn-out is in the form of a slot, not wider than the original hole diameter, but four or five times as long.

The electron gun proper has delivered beams of 33 kW at 165 kV into a beam catcher, which was tightly coupled and was under a semi-vacuum so that the regular beam exit nozzle could be removed. Beam formation and high voltage stability have proved excellent. Replacement or cleaning of the

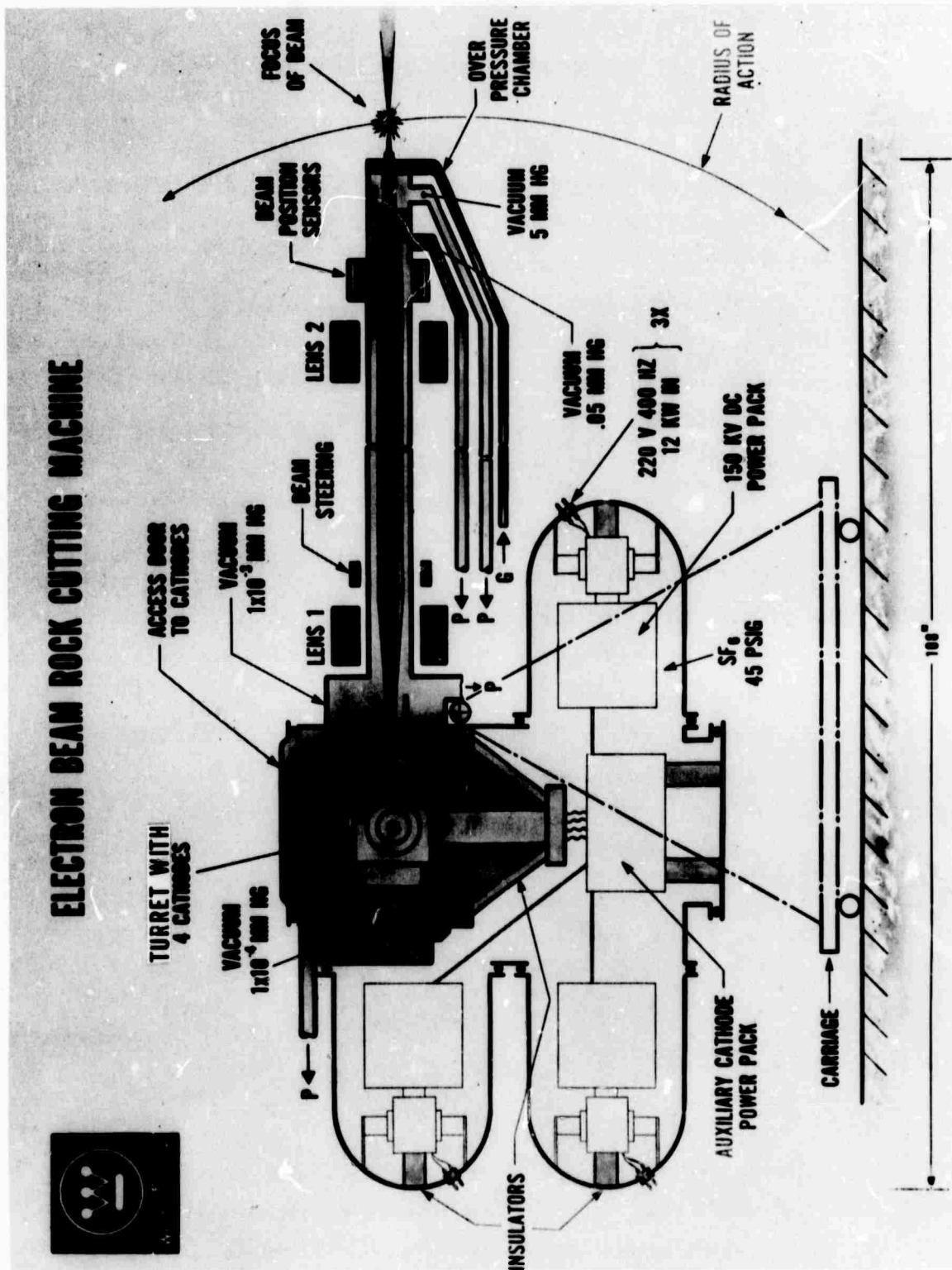


Figure 2-1. Cross-Section Sketch of Electron Beam Gun

high-voltage insulators has not been required since the initial installation. Approximately 400 hours of high-voltage time and 150 hours of beam time have been logged on the machine to date.

The multiple cathodes in the turret have been routinely moved in and out of operating position without alignment problems. Auxiliary power supplies (cathode heater and grid bias), surge limiting resistors, high-voltage metering resistors, spark gaps, isolated drives for turret and bias, etc., have worked satisfactorily since the initial installation.

At present, beam position sensors and a closed-loop beam positioning system are being installed. These are expected to permit continuous operation at higher powers. However, these installations will require another two months to complete.

Figure 2-2 shows the front end of the gun facing a water-cooled beam catcher (Faraday cup) as used for the initial beam alignment. The small plate, visible on the front of the gun, holds the beam exit nozzle and measures 2 inches square. The inside of the catcher is at incandescent heat from the previous beam input, and it illuminates the beam exit nozzle and its surroundings. A bright white coat of molybdenum oxide enhances this effect; it is produced in the catcher which is lined with a molybdenum tube to withstand the high beam power without melting.

Figure 2-3 shows a block of silt stone (copper ore from northern Michigan) in front of the gun before and after piercing and cracking. The lower picture is a view from below the gun. Two piercing cavities shown were produced in about 20 seconds and 60 seconds, respectively, and they led to a spontaneous breakage of the rock.

No attempt has been made to evaluate the results of these initial tests in a systematic manner. Neither these tests nor the above-described developments on the electron gun were charged to the contract.

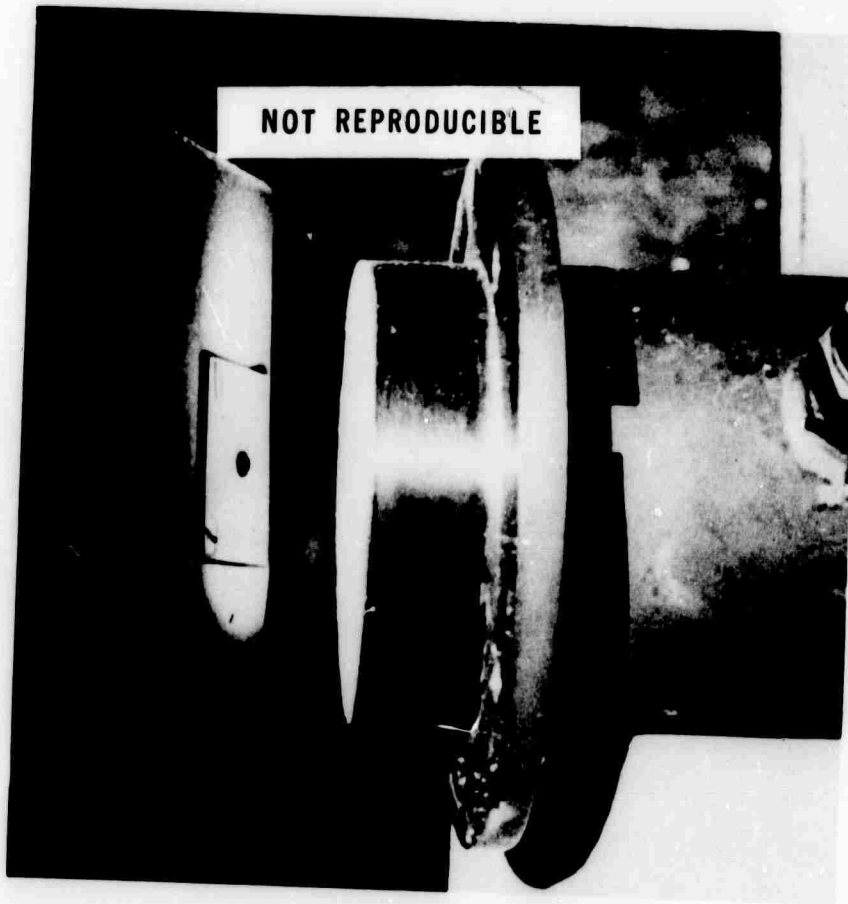
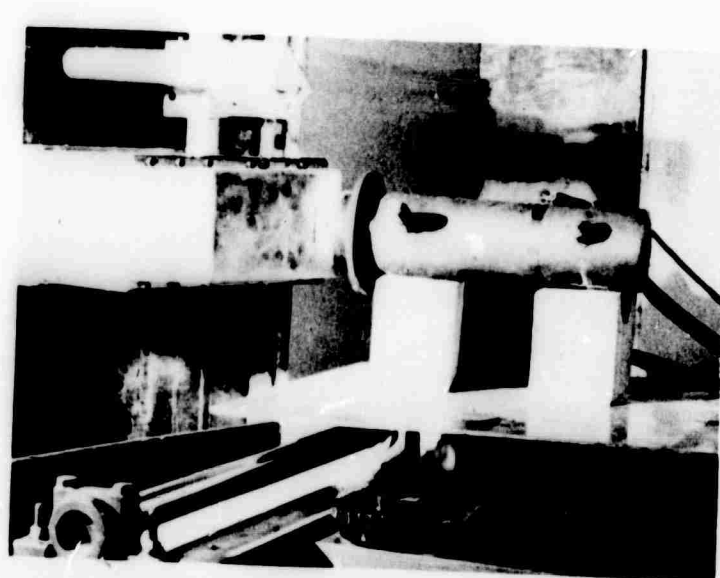


**Figure 2-2. Front End of Electron Beam Gun
Facing Water-Cooled Beam Catcher
Used for Initial Alignment**



Figure 2-3. Electron Beam Gun in Front of
Siltstone (Copper Ore) Before and
After Piercing

2.2 SUPPORT EQUIPMENT

Support equipment for the EBG consists of the gun carriage, the vacuum system, and the electrical power supply system. Except for the motor-generator sets required in field operations, the vacuum system and electrical system existed as laboratory equipment prior to start of work under this contract. Thus, the principal task in this area is the design and manufacture of a carriage to support, position, and manipulate the gun during field test operations. The design task was completed in April 1971. A complete design description appeared in the First Quarterly Report (Ref. 2, p. 2-6). The manufacturing portion of the task was begun, and the completed carriage was delivered to Westinghouse in mid-June 1971.

Work on the carriage since delivery has consisted of completing the electrical and control systems, conducting an operational test of the carriage, and making minor modifications as a result of deficiencies observed in the tests. In-plant testing of the EBG carriage is subdivided into two categories: (1) an initial phase using a mock-up of an EBG, and (2) a final phase to verify operation of the carriage in conjunction with the 36-kW EBG. The first results of the initial phase testing were reported in the Second Quarterly Report (Ref. 3, pp. 2-1 to 2-7). The results of the remaining initial phase tests are described below.

2.2.1 Carriage Test Procedure

Tests were conducted to verify proper operation of the carriage hydraulic system and controls and to determine velocities of motion resulting from various hydraulic system adjustments. To simulate the operational configuration of the carriage with the EBG installed, an EBG mock-up was constructed and installed on the carriage for the preliminary tests. This mock-up, made of concrete and steel pipe, approximates the 36-kW EBG in weight, overall dimensions, and center of gravity location as indicated in Table 2-1.

Table 2-1
COMPARISON OF 36 KW EBG AND MOCK-UP EBG

	<u>36 KW EBG</u>	<u>Mock-up</u>
Weight	1500*	1474
Moment due to CG Location	18,000 in.-lb.	15,500 in.-lb.

The carriage is capable of moving the gun along the x, y, and z axes and in the rotational modes of pitch and yaw. Axis orientation and rotational modes are indicated in Figure 2-4. Motion in each of the five modes of operation is accomplished using linear or rotary hydraulic actuators with velocity control in all modes except the z axis achieved through the use of temperature and pressure compensated flow control valves. Velocity control in the z-axis mode is achieved using an uncompensated variable orifice flow control valve.

2.2.2 Carriage Test Results

Measurements of linear and rotary full stroke displacements were made for each mode of operation. Each of the actuators was then cycled at several different flow control valve settings. The time required for actuation at each setting was measured and recorded.

An additional test was conducted to determine the amplitude and frequency of vibration or beam oscillation present at the end of the gun transfer column. No mention was made in the design requirements of vibration limits, but this was subsequently determined to be an area of concern. Horizontal and vertical vibrations were measured at several flow control valve settings for each mode of operation using MB velocity pickups in conjunction with an MB meter and an oscilloscope.

Actuation Velocities. Times required for full-stroke actuation for various valve settings were used to calculate velocities at the gun exit nozzle.

* The 1500-pound weight was a very conservative early estimate of the gun weight. Actual weight is approximately 975 pounds.

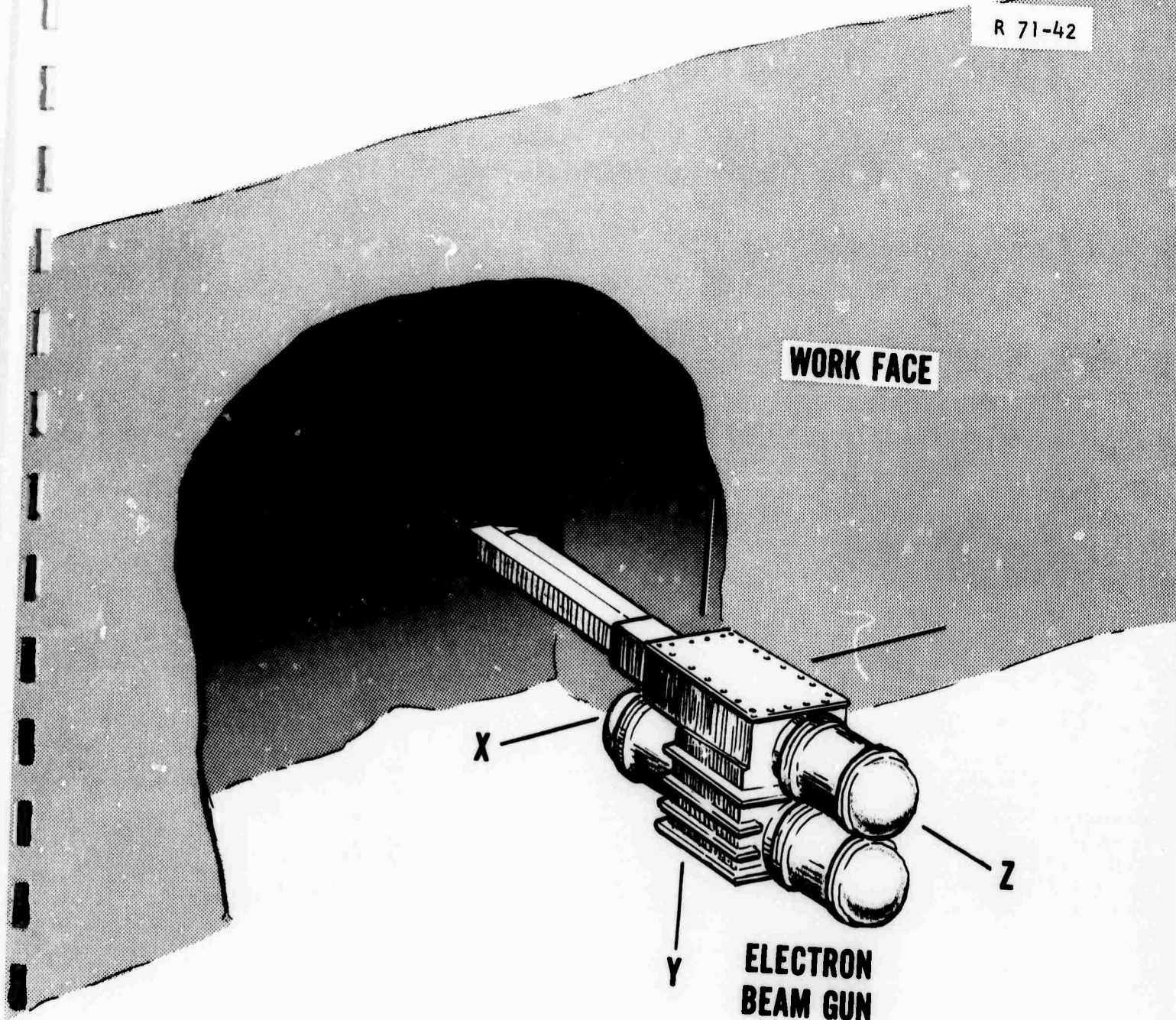


Figure 2-4. Axis Orientation and Rotational Modes
for Electron Beam Gun

Velocities for each mode of operation were plotted against valve opening (see Figures 2-5 through 2-8).

Temperatures. Hydraulic fluid temperatures were recorded throughout the test. The fluid temperature repeatedly reached the maximum allowable temperature of 150° F after about 4 to 6 hours of continuous operation; test operations had to be halted to permit the system to cool.

Vibration. Amplitude and frequency of horizontal and vertical exit nozzle vibration were measured and recorded during each mode of operation at various flow control valve settings. Both amplitude and frequency appear to be independent of actuation velocity. Frequencies were 3 to 4 cps in the horizontal direction and 8 to 10 cps in the vertical. Amplitudes (peak to peak) varied from 0.001 inch to 0.01 inch with averages from 0.0005 inch to 0.001 inch.

2.2.3 Conclusions and Recommendations

General Performance. The electron beam gun carriage performs as required by the design requirements specification except for the irregularities in velocity control and the problem of hydraulic system overheating. No anomalies were noted during operation, and the only construction discrepancy noted was the use of fixed elbow hose connections in the hydraulic system when swivel elbows had been called for on the carriage procurement drawings. Replacement of the fixed elbows with swivel elbows is recommended.

Actuation Velocities. The specification requires actuation velocities in all modes to be variable within the range of 0 to 30 inches per minute. The X- and Y-axis control systems perform in accordance with the specification requirements except for some irregularities which appear on the velocity plots as apparent decreases in velocity resulting from an increase in valve opening. This behavior is attributed to changes in oil temperature and viscosity.

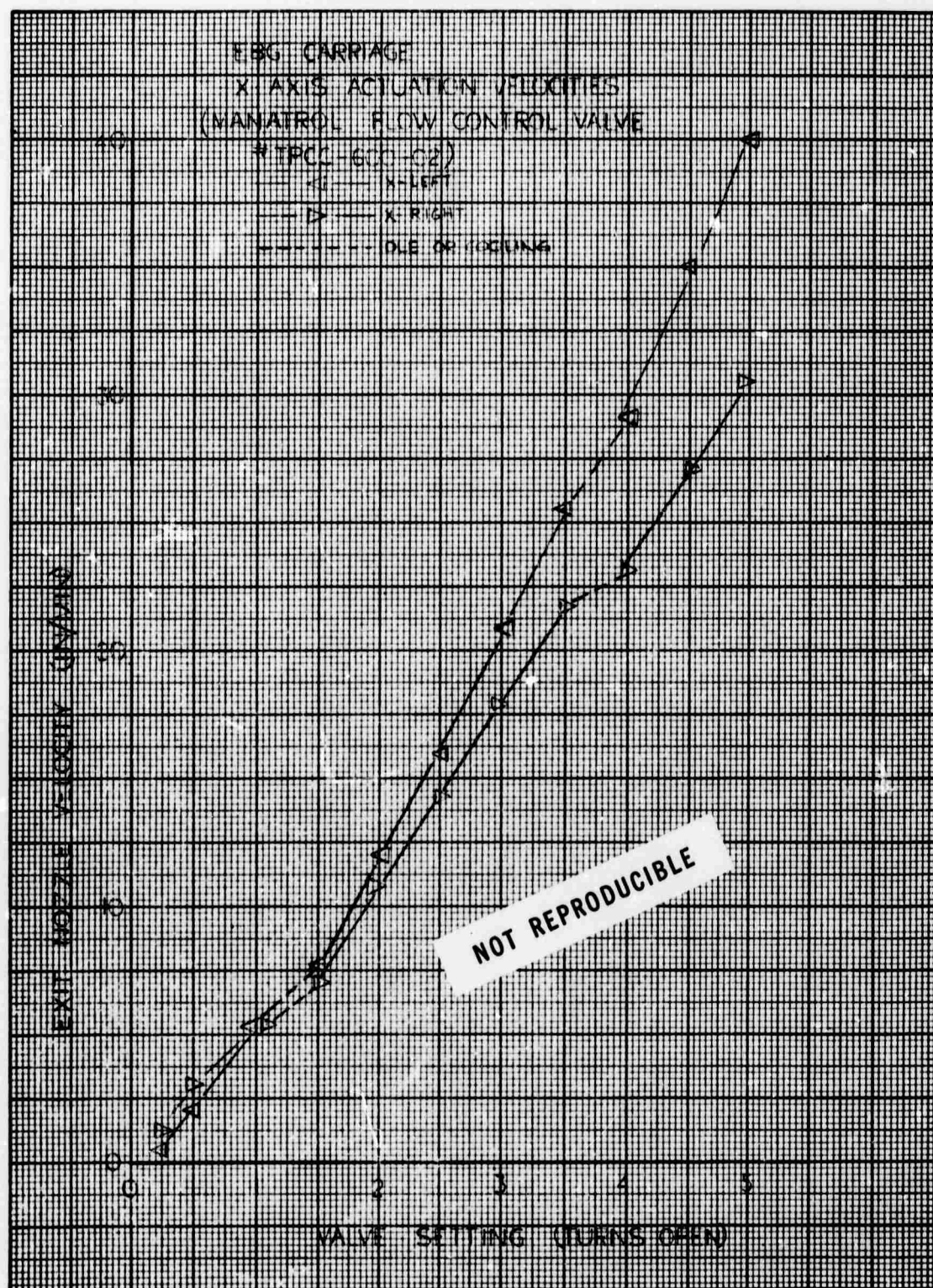


Figure 2-5. EBG Carriage — X-Axis Actuation Velocities

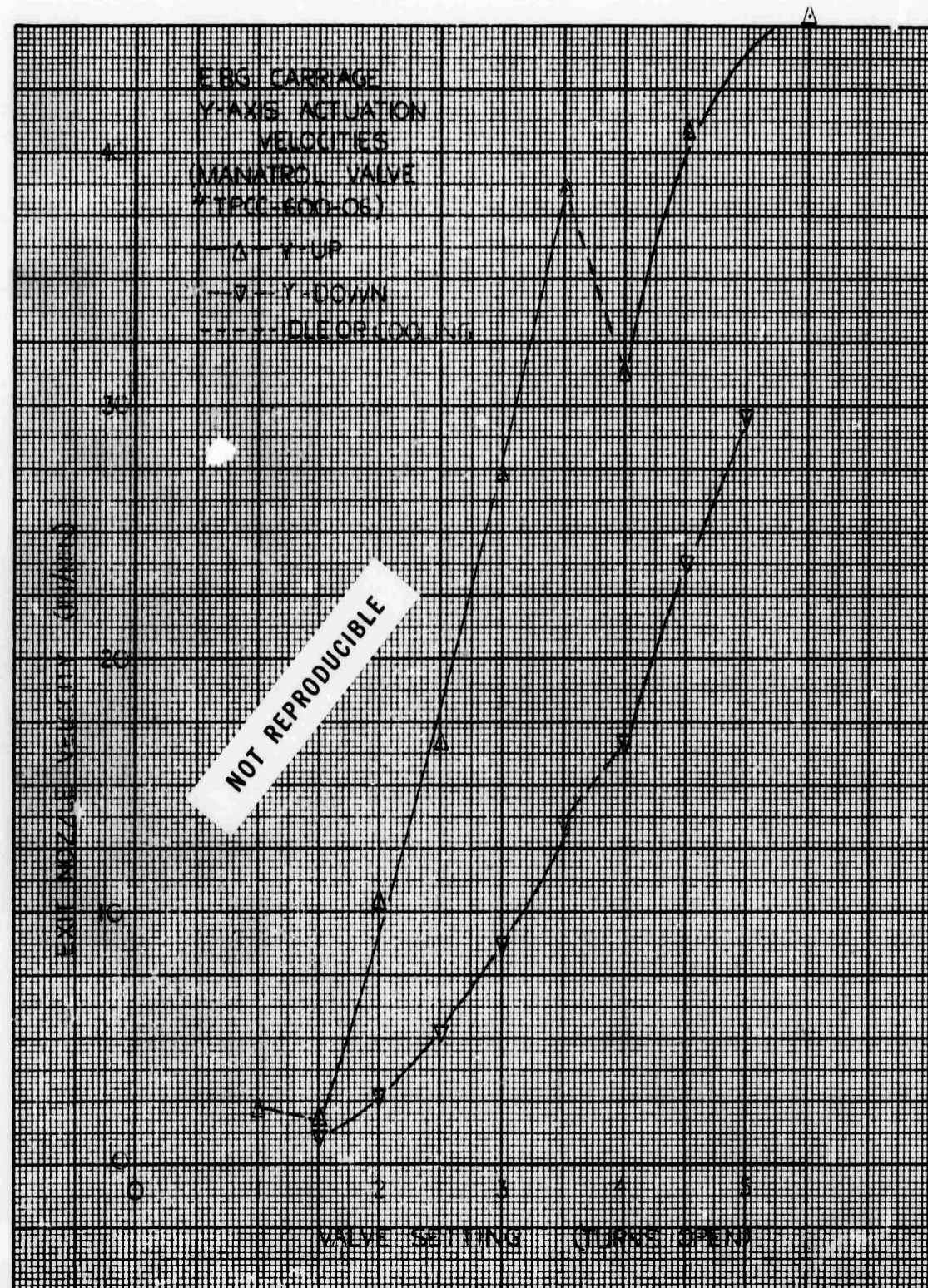


Figure 2-6. EBG Carriage — Y-Axis Actuation Velocities

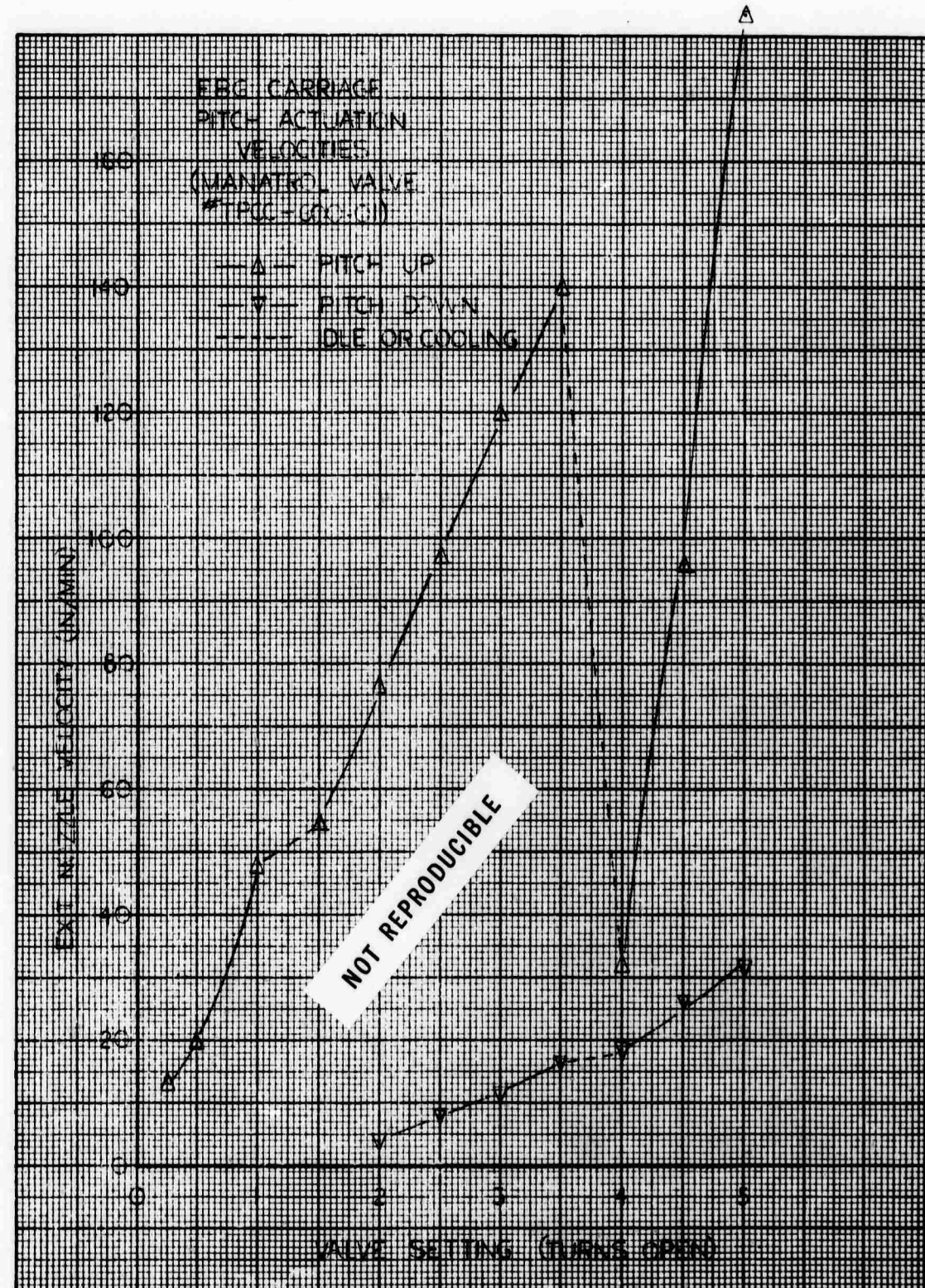


Figure 2-7. EBG Carriage — Pitch Actuation Velocities

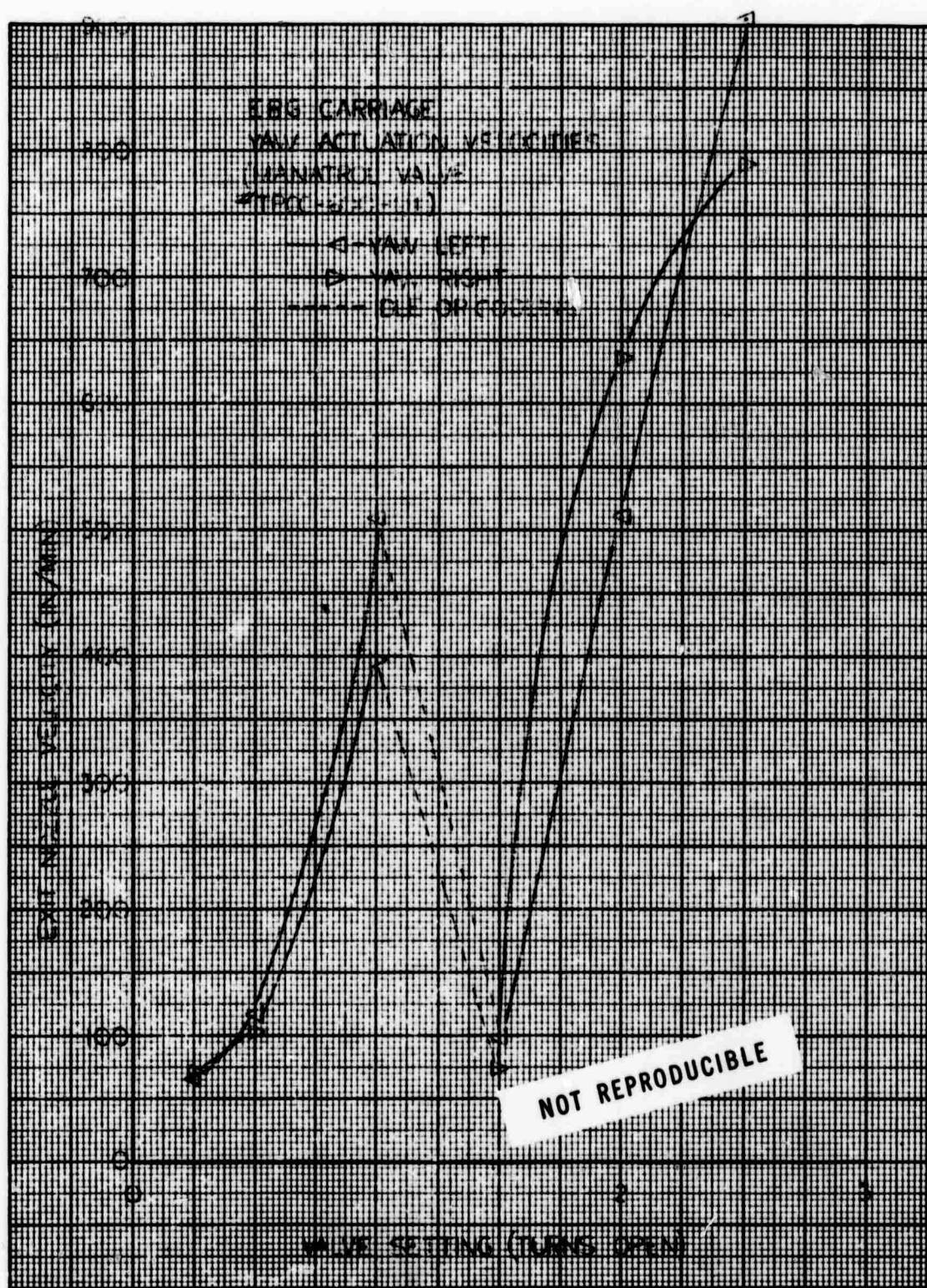


Figure 2-8. EBG Carriage — Yaw Actuation Velocities

Actuation velocities and their control in the pitch and yaw mode are less satisfactory. In the yaw mode, performance was characterized by very high velocities, varying from 67 inches with the valve 0.25 turn open to 900 inches per minute at 2.5 turns open, and by large irregularities in flow resulting from temperature changes in the hydraulic fluid. The manufacturer's specification for performance of the yaw and pitch circuit flow control valves states that they will maintain constant flow over a pressure range of 70 to 3000 psi with a ± 1.0 percent variation in flow, and over a temperature differential of 60° F with ± 2.5 percent variation in flow, in the flow range from 0 to 25 cubic inches per minute. To achieve operation at the desired velocities, the flow controls must operate properly in the bottom 2 percent of the flow range, and they are apparently not capable of this performance. A possible remedy, which may be employed to achieve more precise control in the yaw circuit, would require replacement of the present direct coupling of the actuator to its driven mechanism with a chain or gear drive with at least a 2:1 reduction.

Pitch circuit performance is also characterized by high velocities in the "up" direction and by very low velocities in the "down" direction. Velocities measured in the "up" direction varied from 13.8 inches per minute at a valve setting of 0.25 turn to 185 inches per minute at 5.0 turns open. These velocities correspond to flow rates of 7.7 cubic inches per minute and 104 cubic inches per minute, respectively. Since the maximum flow rate for this valve is 25 cubic inches per minute, the flow control valve is apparently defective. The pitch "down" circuit provides satisfactory velocity control, except that motion was extremely slow until the valve was opened 2.0 turns.

The flow control valve manufacturer has agreed to replace the defective valves. They will also test valves to find two that operate satisfactorily in the lower portions of their flow range. These will replace those presently in the yaw circuit.

Temperature. The maximum permissible operating temperature for the carriage hydraulic system is 150° F. This temperature was reached several times during the test, necessitating a halt in test operations to permit the system to cool to an allowable operating temperature. The temperature fluctuations also have a pronounced effect on flow control valve performance. For these reasons, installation of an air/oil or water/oil heat exchanger is recommended to maintain a maximum fluid temperature of approximately 100° F. Rough heat load calculations indicate that the required heat exchanger should have a maximum capacity of removing 60 btu/minute from the hydraulic fluid returning to the reservoir. The actuation velocity tests should be repeated after installation of a heat exchanger and replacement of defective valves.

Vibration. Amplitudes recorded during the vibration test remained constant at several valve settings and appeared to be affected only by background vibration, such as that caused by motion of heavy machinery in the adjacent area. These inputs, transmitted through the concrete floor of the test area, resulted in large response motion of the carriage and test weight. In field tests, this will not be a problem and the 0.0005 inch to 0.001 inch amplitudes recorded as steady-state vibration may be considered negligible.

R 71-42

3. FIELD TESTS

No effort was performed in this area during the third quarter.

4. THEORETICAL STUDIES

4.1 PIERCING ROCK WITH THE ELECTRON BEAM

The piercing process has been described in the First Quarterly Report (Ref. 2) and elsewhere. The following discussion will refer to some aspects which have been studied more recently, e.g., the importance of the initial beam aperture angle. As originally expected, none of these initially neglected factors are of any great importance.

High-powered, focused, electron beams can quickly vaporize deep, narrow cavities in rock. This process is made possible by the high power density at the center of the beam together with the low thermal diffusivity of the rock. The piercing occurs because of intense thermal energy generated from the kinetic energy of the electrons as they bombard the rock face at the bottom of the growing cavity. When the electrons hit the rock, the energy at the center of the beam is delivered so quickly that only a small portion of it can dissipate by heat conduction into the rock (a quasi-adiabatic condition (Ref. 1)). The remaining major portion of the energy causes extreme local heating, which melts and vaporizes material off the cavity bottom and thus extends the cavity's depth.

The penetration speed starts out initially very high (typically 2.5 inches per second at 9 kW) and decreases with increasing depth because of a degradation in peak beam power density suffered as the beam travels the ever increasing distance to the bottom of the cavity. This distance continues to increase because the electron gun muzzle is much too wide to fit into the cavity and therefore cannot follow the receding rock face. The degradation of the peak power density is due primarily to multiple scattering of the electrons by the gas and by the vaporized rock molecules in the cavity. Although the scattering process absorbs only a small fraction of the electron energy, it nevertheless causes the diameter of the beam to broaden and therefore causes the power density at the center of the beam to diminish. Accordingly, as the cavity grows deeper, the power per unit area hitting the bottom decreases, and thus the growth rate of the cavity also decreases.

Although the cavity diameter also grows with time, it does so more slowly than the depth. At the widest point, usually about half-way down the cavity, the diameter is typically only 1/4 the depth. Its slow growth rate is a result of the power striking the walls being much less intense than that hitting the cavity bottom. The walls are heated only by the relatively few electrons that are scattered out of the main beam and by the transfer of a certain amount of thermal energy from the jet of hot gas vaporized off the cavity bottom and shooting out of the top. Since the power hitting the walls is comparatively low, the energy is deposited sufficiently slowly that a substantial fraction of it is carried away by heat conduction into the rock. The quasi-adiabatic condition is not satisfied. Accordingly only a portion of the relatively low power to the walls is available for vaporizing away material, i.e., available for expanding the cavity diameter. In fact, one finds the walls covered with a layer of often viscous molten rock through which heat flows into the solid rock and sets up steep temperature gradients. It is these temperature gradients that produce the severe thermal stresses on which the rock-cracking process depends.

Details of the theoretical description of the piercing process appeared in the First Quarterly Report (Ref. 2, p. 4-3). The process is dominated by two effects: (1) the quasi-adiabatic removal of material from the bottom of the cavity, and (2) the decrease in peak beam power density with distance because of multiple scattering. However, there exist other processes, which were neglected in the first report, but which also tend to degrade the beam before it hits the rock. The effects of several of these processes have been estimated recently, and found to be quite small for the power levels and distances involved. For example, because of the low gas density in the cavity, energy loss from the beam through ionization, i.e., through collisions with the planetary electrons of gas atoms, causes a loss of only about 3 percent in the energy of the average individual electron before it reaches the bottom of a 5 inch-deep cavity. Another example is the broadening of the beam and consequent reduction in power density expected from

the initial angular divergence of the beam at the exit nozzle of the gun as caused by the electron optics system. This effect is also small. An initial beam envelope half angle of as much as 3 degrees is responsible for only 6 percent of the beam diameter near a rock face 1/2 inch from the gun. This contribution continues to drop with distance from the gun to only 3 percent at the bottom of a 5-inch-deep cavity. That the initial beam divergence has such a small effect is a consequence of the random walk process of the multiple scattering. For relatively small initial beam divergence angles, it is appropriate to combine the effects of divergence and scattering by adding the two contributions in quadrature. Consequently, the effect of scattering almost entirely masks the effect of the initial beam angle. Accordingly, as long as the beam's initial angular divergence is sufficiently small, its actual value has only a small influence on the beam divergence outside the gun.

Another energy loss mechanism, which turns out to be small, is bremsstrahlung (energy loss to x-rays in the electromagnetic field of the atomic nucleus). It becomes important only at electronic energies greater than about 7000 keV, i.e., much greater than the 150 keV of the electron-beam rock cutter. In fact, measurements show that only about 1/4 percent of the total incident beam power is lost to the combination of bremsstrahlung and x-ray line radiation. However, at the point where the electrons hit the dense molten rock or the solid rock of the walls or the bottom of the cavity, energy loss through ionization becomes the dominant effect. It is through this mechanism that the electrons give up nearly all of their kinetic energy to the material, and thus produce the intense heat needed for piercing. In losing its energy, an individual electron characteristically penetrates 3 to 4 miles into the molten or solid material, and although backscattering out of the material is possible, only about 5 percent of the incident power is reflected in this fashion.

Three effects have not been considered in formulating the theoretical model for piercing: (1) the spatial variation of temperature, and therefore of

gas density, in the cavity as a result of nonuniform heating by the beam; (2) the motion of the molten rock within the cavity as a result of boiling and the force of gravity; and (3) the variation in beam power density caused by macroscopic electromagnetic fields in the beam path caused by the beam's interaction (e.g., ionization) with the material. The assumed Gaussian beam profile, on which the calculation depends, itself depends on the gas density being constant. However, the gas at the center of the beam is heated much faster than that near the edges and, to the first approximation, is therefore less dense; thus, the assumption of uniform density is violated. On the other hand, strong convection currents together with jets of vaporized rock are presumed to break up any steep temperature gradients that form within the confines of the cavity and thus maintain the density more or less constant. As for the effect of molten rock, the thickness of the liquid layer is only a small fraction of the cavity diameter in most cases. It is true, however, that for vertical cavities drilled downwards, liquid from the cavity walls flows to the bottom where it must be continuously removed by the beam. Experimental confirmation of this effect has appeared during laboratory tests, where the depth of vertical cavities reached a maximum limit, in violation of the theoretical prediction. Finally, there is no indication of any macroscopic electromagnetic effects that would cause the theory to be contradicted by our experimental data. Discussion of the laboratory tests and the degree to which they support the theoretical calculations appeared in Reference 2, Section 5.

4.2 TEMPERATURE DISTRIBUTION

In calculating the thermal stresses in the rock, a reasonable yet tractable model has been used to approximate the cavity shape and to give the temperature distribution within the solid rock (see Ref. 3, pp. 4-2 through 4-8). The simplifying assumptions include:

1. The cavity is cylindrical with a hemispherical bottom. The final depth is 4.2 times the diameter. (The final depth as a function of piercing time is calculated according to the piercing theory of Ref. 2, Section 4).
2. For calculating the heat flow into the rock (and therefore the temperature), the walls of the cavity are considered as a moving isotherm held at the melting temperature of rock.
3. The moving isotherm, a cylinder with a hemispherical base, moves only downward, i.e., it has a constant diameter equal to that which the cavity has when the beam is eventually turned off. The depth grows with time, but the diameter does not.
4. The thermal diffusivity is independent of temperature. The value chosen as typical for rock is 8×10^{-4} square inches per second.

With these assumptions, it is possible to determine an approximation to the temperature distributed within the rock by a simplified calculation. In a plane at each depth below the rock surface, the temperature is taken to be given by the solution to the time-dependent heat equation appropriate for an infinitely long cylinder of constant temperature and radius imbedded in an infinite medium of constant thermal diffusivity. The value of the time used in the solution depends on the depth. Planes at greater depths are heated for shorter times than those near the outer surface of the rock. Since the cavity bottom advances into the rock faster than the temperature can propagate, the time appropriate for a given depth is taken to be the elapsed time from when the cavity passes through that depth to when the beam is turned off. The cylinder radius used in the solution at the given depth is given by the radius of the full-grown cavity at that depth.

Thus, this procedure gives a temperature distribution that is wide near the outer surface of the rock and decreases in width with depth until it becomes zero at the cavity bottom (see Ref. 3, Fig. 4-7). By keeping the cylinder radius constant in time, the calculation procedure is simplified, as it avoids the complication of a moving cylindrical boundary advancing into the heated rock.

The temperature calculation, however, overestimates the distance into the rock to which the heat actually penetrates. First, the radius of a real cavity does, in fact, expand with time and at a speed comparable to the speed of heat conduction. Therefore, by the time the radius reaches its full size, it overtakes much of the thermal energy that diffuses into the rock. However, it has been assumed that the heat begins diffusing from a point located at the maximum radius of the cavity and that none of the heat is overtaken. Second, the thermal diffusivity does not remain constant with temperature but, for example, can decrease by a factor of 5 as the temperature goes from 20° C to 600° C (Ref. 4, p. 709). The value of diffusivity chosen corresponds to 200° C for Dresser basalt or 280° C for Charcoal granite. Yet, for example, with these two rocks, the thermal diffusivity drops at elevated temperatures (i.e., greater than 600° C) to half the value used. Such a drop will inhibit heat flow from the hot cavity and will therefore also restrict the distance the heat propagates.

It is certainly possible to improve the model for calculating the temperature distribution by numerically solving the three-dimensional, time-dependent, differential equation for heat conduction for the case of a cavity growing in diameter as well as in depth and for a thermal diffusivity that changes as a function of temperature. However, to be complete, the calculation should also include the insulating effects of small cracks, which are, in turn, caused by the thermal stresses. Such a calculation is beyond the scope of the present investigation.

Because of the uncertainty in the temperature calculation, it was deemed instructive to look at the effect that a drastic change in the assumed rate of heat propagation has on the calculated thermal stresses in the rock. Accordingly, stress calculations were made for piercing times of 5, 20, and 300 seconds for which the thermal diffusivity was assumed to be 4×10^{-4} square inches per second, i.e., just half the value used in the original calculations. The procedures followed were identical to those used with the original diffusivity as described in the Second Quarterly Report (Ref. 3, Section 4.5). The results were similar to those of the original calculation for corresponding piercing times. The isostress plots had nearly the same shape in both cases, although halving the thermal diffusivity reduced the width of the stressed region by 15 to 20 percent. However, there was on the average no significant decrease in maximum value of tensile stress calculated for the three piercing times.

4.3 ROCK FAILURE

Although the rock is expected to fail under tension, it is difficult to predict the time, location, and configuration of the fracture surface. In fact, there is actually no unique tensile strength for a given type of rock. As pointed out by Jaeger and Cook (Ref. 5, p. 140), "the tensile strength of rock is more variable and more influenced by specimen size than any other mechanical property of rock."

A promising line of reasoning is based on the proposition that the variation in tensile strength with sample size depends on statistics. The larger the volume under tension, the higher the probability of initiating a failure somewhere in the volume. A situation of this type can be described by a version of the so-called weakest link theory. Jaeger and Cook (Ref. 5, p. 186) discuss such a formulation by Weibull (Ref. 6), which is the basis for the following argument. If one calls ΔP the probability that a failure occurs within a small volume of rock ΔV , then a probability density dP/dV can be defined as a function of position and stress such that, for small volumes, the failure probability is

$$\Delta P = \frac{dP}{dV} \Delta V$$

The probability S that the whole rock survives with no failure is given by the product of the survival probabilities $1 - \Delta P$ of all the volume elements making up the entire volume of the rock.

$$S = \prod_{i=1}^m \left(1 - \frac{dP}{dV} \Delta V_i\right)$$

Taking the logarithm of both sides converts the product into a sum, which for the condition $(dP/dV)\Delta V_i \ll 1$, becomes

$$\ln S \approx - \sum_{i=1}^n \frac{dP}{dV} \Delta V_i$$

Letting n go to infinity as ΔV_i goes to zero converts the sum to an integral, and the failure probability $P = 1 - S$ becomes

$$P = 1 - \exp \left[i - \int_v \frac{dP}{dV} dV \right]$$

This expression gives the probability that a failure will occur somewhere within the rock. For simplicity, Weibull assumes a power law for dP/dV given (in the notation of Hudson (Ref. 7)) by

$$\frac{dP}{dV} = \left(\frac{s}{s_0} \right)^m$$

such that

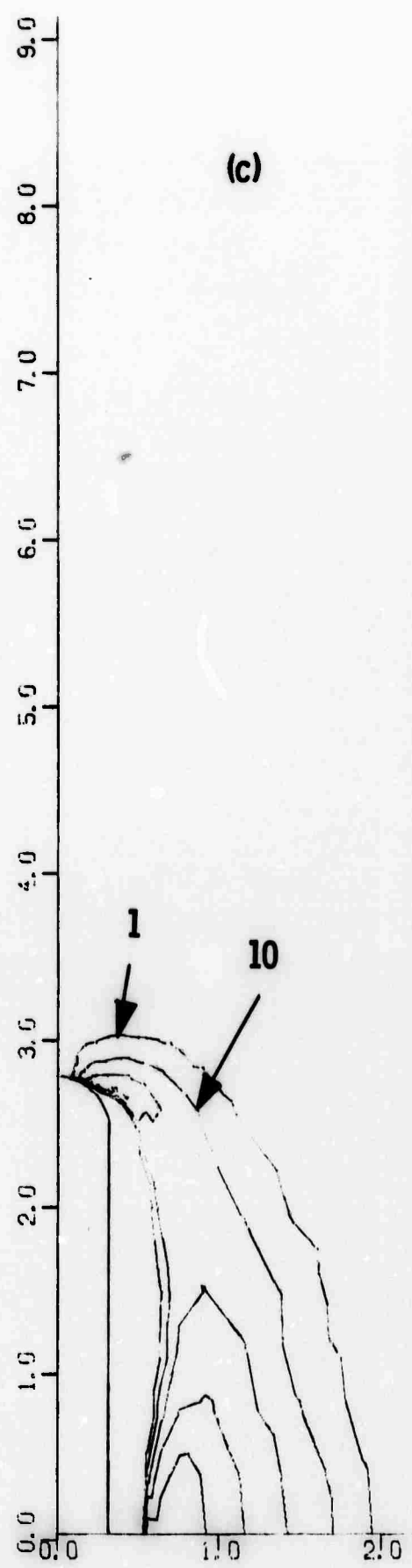
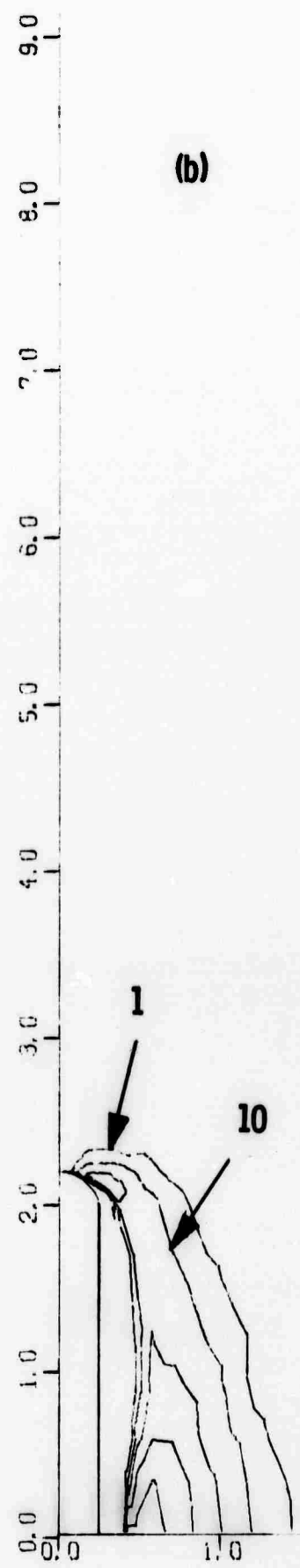
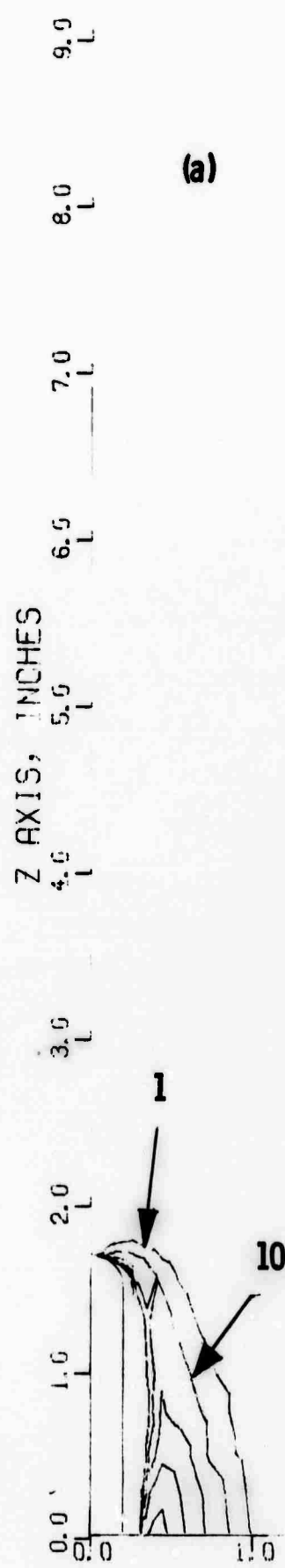
$$P = i - \exp \left[- \int_v \left(\frac{s}{s_0} \right)^m dV \right]$$

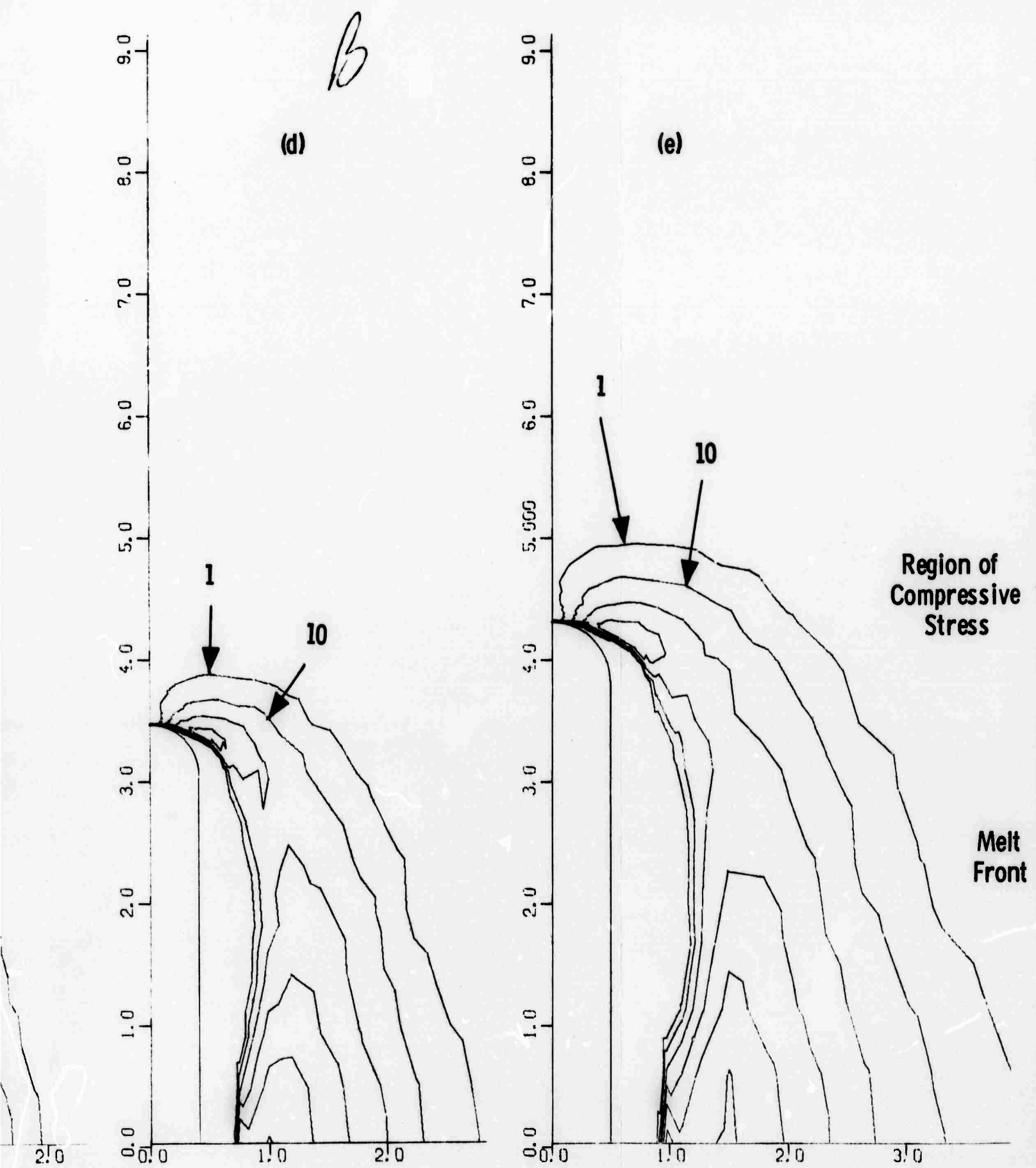
where m and s_0 are constants depending on the type of rock, and s , a function of position, is the maximum principal tensile stress (in psi). Although Hudson found s_0 and m to vary somewhat with volume, it is instructive to use some typical values that he obtained from measurements on red granite, i.e., $s_0 \approx 2000$, and $m = 6$. These values together with the calculated stresses as a function of position and time (Ref. 3, Section 4.5) result in plots of probability density shown in Figure 4-i.

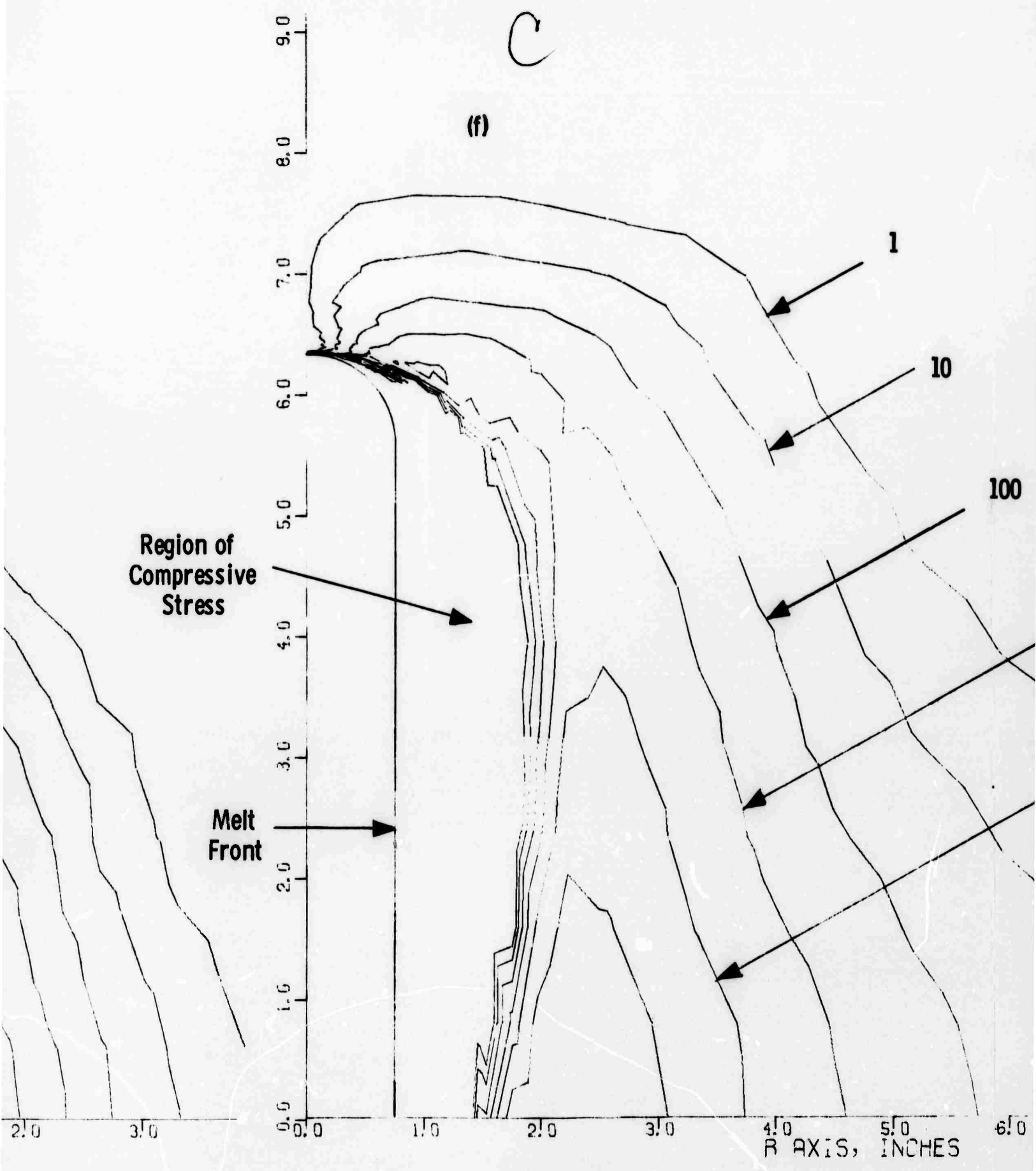
The quantity plotted in Figure 4-i is actually dP/dA , i.e., the probability of failure per unit area rather than per unit volume and is more appropriate for a case with cylindrical symmetry than is dP/dV . The quantity $(dP/dA) \Delta A$ represents the probability that a crack will occur somewhere in a ring of small cross-sectional area $\Delta A = \Delta r \Delta Z$ located at radius r ; dP/dA is given by

$$\frac{dP}{dA} = 2\pi r \frac{dP}{dV}$$

A







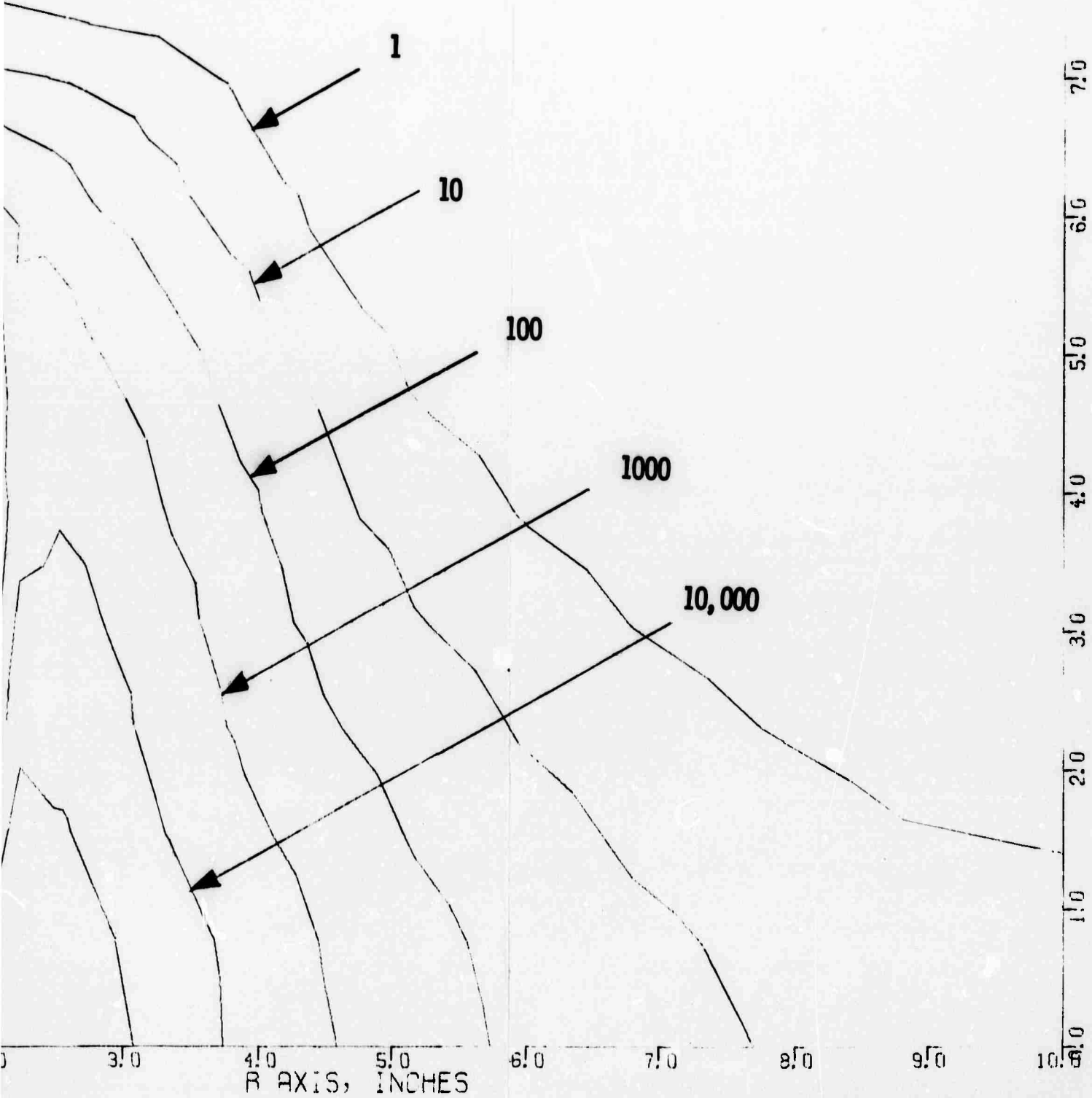
D
0.0
0.5
1.0
1.5
2.0
2.5
3.0
3.5
4.0
4.5
5.0
5.5
6.0
6.5
7.0
7.5
8.0
8.5
9.0
9.5
10.0

Figure 4-1. Failure Probability per Unit Area Caused by Tensile Stress

The contours plotted in Figure 4-1 are for $dP/dA = 1, 10, 100, 1000, 10,000,$ and $100,000.$ Panels (a) through (f) represent piercing times of 4, 10, 20, 40, 80, and 300 seconds, respectively. These results are for a 9-kW, 150-kV beam, with a 1/2-inch standoff distance. The probability P that the rock will crack somewhere turns out to be essentially unity for each of the piercing times considered. The contours in Figure 4-1, however, show graphically the points at which the cracks are most likely to start.

It is apparent from Figure 4-1 that cracking commences as soon as piercing begins and continues with increasing vigor, presumably until the number and/or size of the cracks alter the geometry of the rock so much that there is sufficient stress relief to invalidate the model used for the calculation. By that time, of course, the rock has suffered large-scale failure, which is the objective of the process. However, the details of how and when the large cracks begin to propagate are not yet understood. The degree to which small cracks formed early relieve the stress is unknown as is the effect of these small cracks being overtaken by the advancing front of molten rock. Further study of this subject will be necessary to determine the extent to which such a complicated sequence of events does occur. One would also like to know to what extent such a process would alter the temperature field, and at what point the cracks cease to be localized and propagate far from the cavity.

It is pure conjecture at this time, but the occurrence of macrocracks may have nothing to do with the microfracturing near the melt-front and is only determined by the heat flow and stresses in the deeper layers of the solid rock. Such a situation would be in agreement with our observations and the stress field data from our idealized calculations.

The above discussion completes the theoretical studies under this contract, except for a detailed presentation in the final report.

R 71-42

5. LABORATORY TESTS

No laboratory tests were performed during the third quarter.

6. REFERENCES

1. B. W. Schumacher: "Electron Beam Cutting of Rocks and Concrete," Electron and Ion Beam Science and Technology, Third International Conference, R. A. Bakish, Ed.; The Electrochemical Society Inc., New York, 1968, pp. 447-468. Also E/MJ, June 1969, pp. 116-119.
2. Westinghouse Missile Launching and Handling Dept., Sunnyvale, Calif., R 71-16, First Quarterly Technical Report (1 January - 31 March 1971) - Use of Electron Beam Gun for Hard Rock Excavation, 30 April 1971.
3. Westinghouse Misslile Launching and Handling Dept., Sunnyvale, Calif., R 71-35, Second Quarterly Technical Report (1 April - 30 June 1971) - Use of Electron Beam Gun for Hard Rock Excavation, 30 July 1971.
4. K. Thirumalai, Proceedings, Eleventh Symposium on Rock Mechanics, June 16-19, 1969, The American Institute of Mining, Metallurgical, and Petroleum Engineers, Inc., New York, 1970.
5. J. C. Jaeger and N.G.W. Cook, Fundamentals of Rock Mechanics, Methuen & Company, London, 1969.
6. W. Weibull, "A Statistical Theory of the Strength of Materials," Ingvetensk. Akad. Handl. No. 151.
7. J. A. Hudson, Proceedings of the Eighth Symposium on Rock Mechanics, September 15-17, 1966, The American Institute of Minlng, Metallurgical, and Petroleum Englnneers, Inc., New York, 1967, p. 162.